Bachelor's Degree, Student Owns Copyright (and using a CC License)

Design and Construction of a Fully Submerged Hydrofoil Drone Boat

By

Jonhenry Poss

Submitted to the
Department of
Mechanical Engineering
In Partial Fulfillment of the Requirements for the Degree of

BACHELOR OF SCIENCE

at the

MASSACHUSETTS INSTITUTE OF TECHNOLOGY

May 2023

Authored by: Jonhenry Poss
                Department of Mechanical
                Engineering May 18, 2023

Certified by: Dr. Franz Hover
                Senior Lecturer, Thesis Supervisor

Accepted by: Christina Spinelli
                Department of Mechanical Engineering Sr. Administrative Assistant

Design and Construction of a Fully Submerged Hydrofoil Drone Boat

by

Jonhenry W. Poss

Submitted to the Department of Mechanical Engineering

ABSTRACT

A remotely operated hydrofoil watercraft was designed and built as a test platform for active electromechanical controls as applied to fully submerged hydrofoils in a form just small and lightweight enough to be tested safely without a human physically at the controls. The goal was to build a watercraft sufficiently large and scalable enough that results obtained from it could be realistically applied to personal hydrofoil vehicles without the danger of a human in the vessel during testing. The project also explores roll dynamics while not on foil.

The vessel was built to a length of 1.53 meters with 0.34-meter masts with servo controlled forward foil and aft flippers. The hull is constructed from lightweight 1/8in plywood with a fiberglass and epoxy composite skin. The foils and masts were 3D printed at low density and skinned with fiberglass. These structures have mechanically performed well, surviving both the hydrodynamic forces and repeated crashes. The foils were designed such that the craft would reach foiling speeds at zero degrees pitch at 4 m/s at a mass of 13.1 kg distributed 70% to the aft foil and 30% to the forward foil. The final weight was 14.1 kg. Working towards digital control, the watercraft is equipped with two ultrasonic sensors for height sensing, with room for expansion, and an inertial measurement unit.

Thesis Supervisor: Dr. Franz Hover
Title: Senior Lecturer

Acknowledgements

Thank you to Dr. Franz Hover who advised this project and put great effort into attempting to limit its scope to a manageable size.

Thank you to the various members of MITERS who put up with me building a boat in our shared workshop.

Thank you to Lili Sun and Rulan Gu, who kept me company on the dock during early morning testing.

Table of Contents

Contents

1 List of Figures

2 Introduction

Hydrofoil boats are watercraft that reduce drag by using underwater wings, called hydrofoils, to lift vessels from the water. This decreases the wetted area of the craft, reducing drag. Fully submerged hydrofoils require control systems to maintain flight. This control system can be mechanical, but the watercraft described in this work is software controlled.
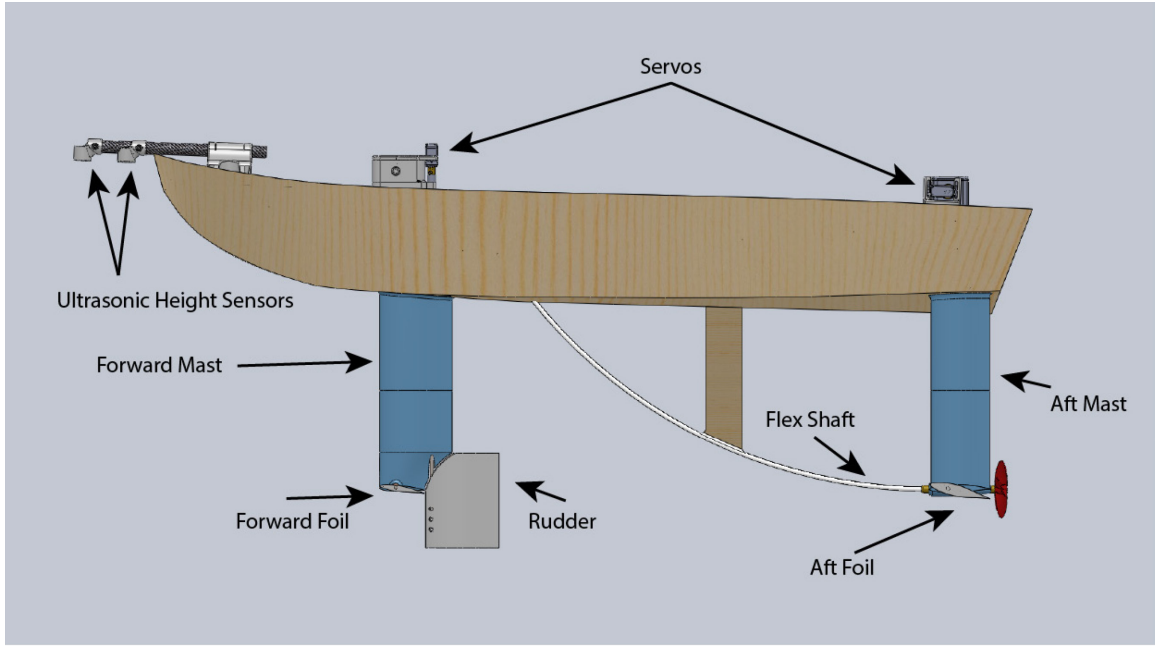
Figure 2.1 In the above image, components constructed from fiberglassed plywood are represented with pine pattern and 3D printed components are pictured in light blue or grey.

2.1 Background
2.1.1 Hydrofoil Vehicles

Fully submerged hydrofoils are a specific form of hydrofoil in which the foils do not pierce the air-water boundary[1]. This improves efficiency over surface piercing foils by reducing the drag caused by contacting the interface. Surface piercing foils are also less subject to the influences of waves at the surface, reducing accelerations and improving the ride [2]. The downside of surface piercing foils is natural instability. Some control scheme must be used to limit the height of the foils and prevent breaching [3].

Hydrofoils are also useful for control of regular planning vessels. Some work has been done to demonstrate the effectiveness of static hydrofoils and hydrofoils with proportional derivative (PD) control to reduce movement in the roll axis resulting from waves or other disturbances [4,5]. With monohull vessels, such as the watercraft described in this article, the roll axis is particularly undamped, leading to the potential for substantial roll movement. This poses a problem for the comfort of passengers, the functioning of instrumentation, and seakeeping. This work continues to explore active foils by characterizing the roll of the hydrofoil in response to the angles commanded to the rear flippers.

2.1.2 Foil Theory
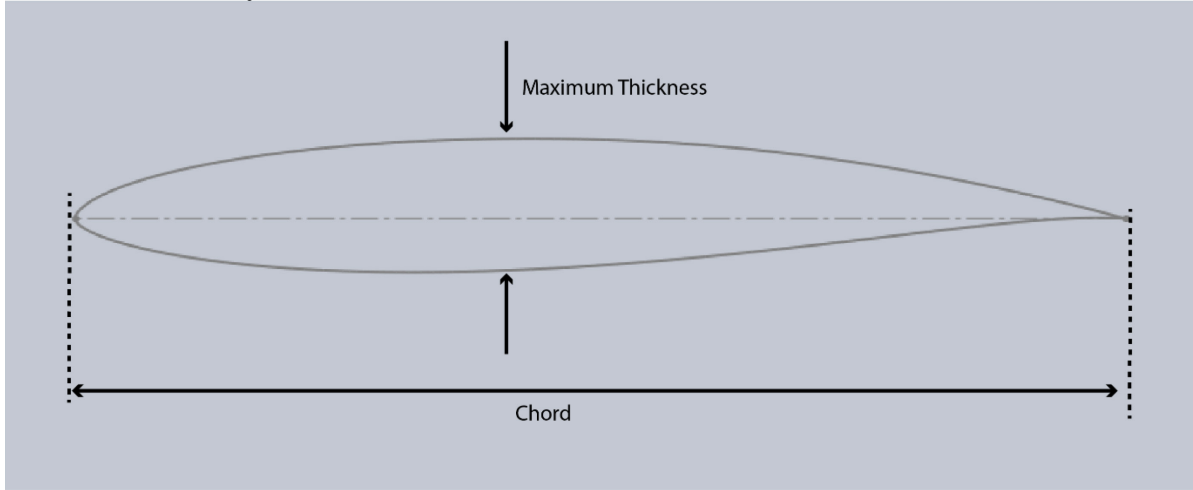
Figure 2.2 Foils area is defined by the chord, which is the tip to tail length of the foil, multiplied by the span, the thickness perpendicular to the profile shown in the figure above.

Foils are aerodynamic shapes that produce lift, a force roughly perpendicular to the direction of motion, when a fluid flows past. In the case of hydrofoil craft, the foil is referred to as a hydrofoil. Lift provided by a foil is given by the equation:

$$Lift = \frac{p}{2} \cdot C_L \cdot U^2 \cdot A$$

Where C_L is the nondimensional lift coefficient and U is the velocity of flow relative to the foil, A is the planform area of the foil, and p is the density of the fluid. Of particular importance is the coefficient of lift. This value is dependent on a complex combination of factors and is often determined experimentally through a range of Reynolds Numbers and angles of attack. The angle of attack is the angle of the centerline of the foil relative to the velocity vector of the fluid [6]. The Reynolds Number is the ratio of inertial forces to viscous forces for a given body and is given by the equation:

$$Re = \frac{\rho U l}{\mu}$$

Where l is the characteristic length of the body, typically chord length for a foil section, and μ is the dynamic viscosity of the fluid [6].

While the weight of the vessel is constant, the lift produced by the foils is dependent on the square of the vehicle's velocity. Therefore, it is necessary to reduce the lift coefficient or area in some way to prevent breaching as the velocity of the boat increases [7]. Some hydrofoil watercraft achieve this by taking advantage of the reduction in lift as the foils approach the fluid interface, though this requires careful tuning and is uncommon. Surface piercing foils passively decrease lift as more of the foil leaves the water, reducing the area [8]. Fully submerged foils, such as those used in the watercraft described in this work, must adjust the coefficient of lift. In this vehicle, this is achieved by rotating the front foil, pitching the entire craft up and down to change the angle of attack of the foils.

2.1.3 Drag

The drag, or energy loss to fluid effect, is the driving factor in the efficiency of vehicles moving through fluid mediums. In traditional watercraft, most drag is accounted for by skin drag and the wave drag. Skin drag is the drag due to the friction of the fluid on the hull. This is dependent on the surface area of the vessel and its speed. Wave drag is the drag caused by the energy dissipated in the creation of waves. Both the leading and lagging edge of vessels create waves as they displace water [9].

The effects of these drag forces motivate the creation of hydrofoil watercraft. Hydrofoils and their masts have substantially lower surface area compared to the wetted area of a traditional hull, reducing skin drag. Wave drag is also reduced, as only the thin, hydrodynamic masts pierce the surface of the water. From this it is also clear why surface piercing foils are less efficient than fully submerged foils; they produce more wave drag due to piercing the surface.

2.1.4 Stability

While conventional vessels have inherent stability due to the buoyant forces of the hull, submerged foils are reliant on control systems to regulate angles and height [2]. The watercraft described in this work was created with the intention of acting as a test platform for the complex problem of control. Hydrofoil vessels generally require active control in the pitch, roll, and heave axis. In this case, control of pitch indirectly controls heave as pitching the hydrofoil up increases the lift produced by the foils. Roll is another important axis during foiling, particularly in turning. Banking into turns reduces side loading on the hydrofoil struts, and provides a more comfortable acceleration [2].

3   Design and Calculations

3.1   Hydrofoil Layout

Hydrofoil vessels typically make use of either the conventional layout, with a large foil forward and a smaller foil aft providing downwards lift, or the canard layout, with the large foil located aft and a smaller foil forward that also provides positive lift. Both layouts provide some amount of dynamic pitch stability.
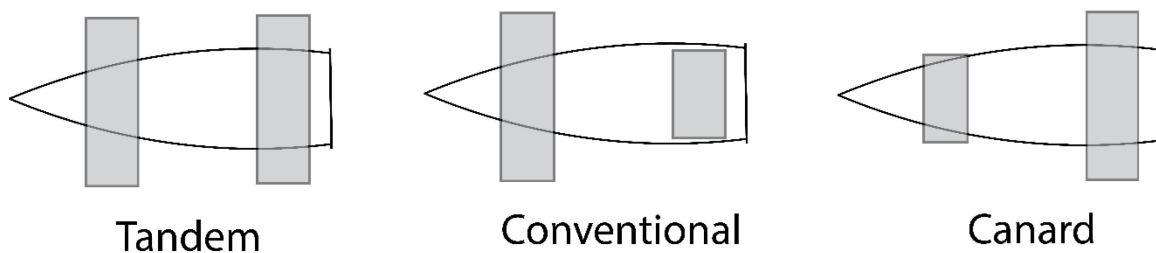
Figure 5.1 Typical foil layouts.

The canard layout was chosen because the larger aft foil provides a robust mounting point for the prop shaft. The efficacy of this design is also well supported by existing hydrofoil vessels, which most commonly follow the canard layout [7]. Having a robust aft foil is important, because the drive shaft is of the flexible variety, and must be supported both at the motor and just forward of the propellor.

3.2 Hydrofoil Profile Selection

Hydrofoil sections serve two distinct functions on the watercraft. The first is the lift producing hydrofoils themselves. The second is the streamlining of the masts. This watercraft was designed as a test platform for software control, not as an experiment in maximizing efficiency. As such, foils were selected based on practicality of manufacturing and use in similar watercraft.

The Eppler E838 was selected for the mast profile from the NACA database [10]. This profile was selected for its high ratio of thickness to chord length, 0.184. This criterion was most important because the mast must be thick enough to accommodate the belt drive system used to control the control surfaces. It is also a symmetric foil, as the masts do not need to generate lift. The lifting foils require an asymmetrical profile to generate more lift. The H005 profile was selected, as it is designed for small, low speed hydrofoils [11].
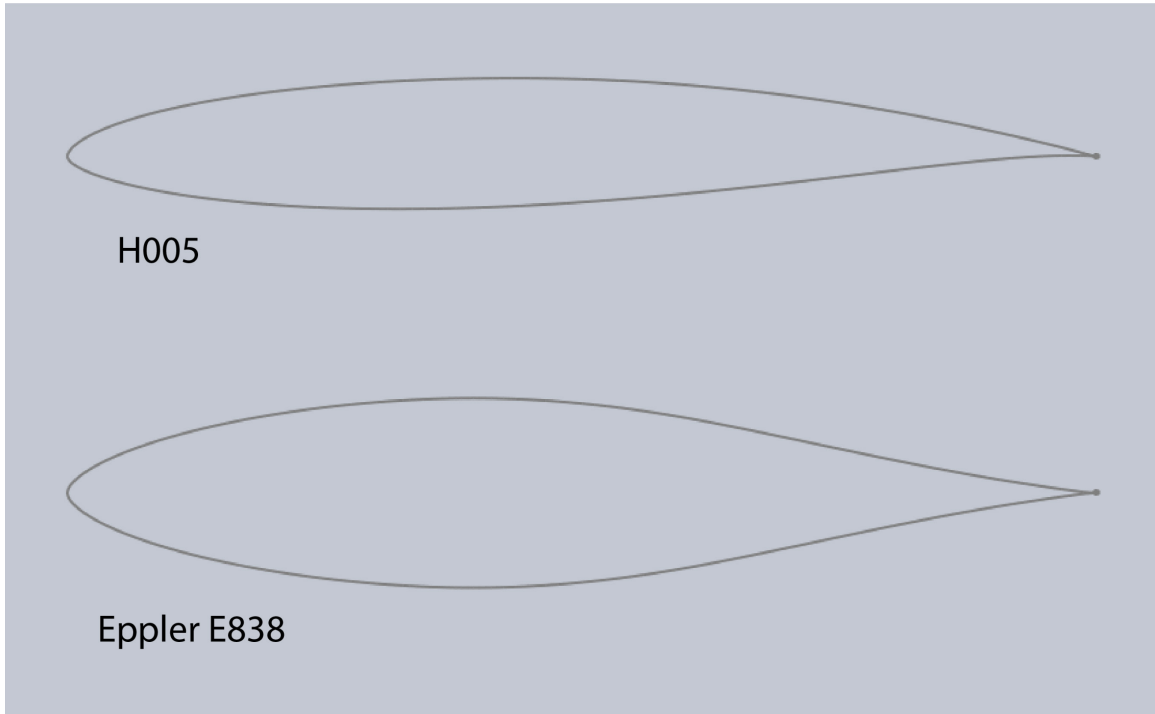
Figure 3.2 The asymmetric foil used for the forward and aft lifting foils and the symmetric foil used for the masts and flippers.

3.3 Lift Calculations

The total mass of the vessel was estimated at approximately 6.5 kg. This was then doubled to 13 kg out of an abundance of caution for discrepancies in mass that might occur due to epoxy-rich fiber glassing and additional features not accounted for in the initial design. At the target take-off speed at 4 m/s, the weight of the hydrofoil must be matched by the lift produced by the hydrofoils in level flight. This force balance is described by the following equation:

$$Mg = \frac{p}{2} \cdot C_L \cdot U^2 \cdot A$$

As a canard, the craft is expected to support 70% of the weight on the rear foil. From the lift equation and the coefficient of lift at zero degrees (0.3), the aft foil must have a surface area of 28042 mm^2. For stability, the front foil must support more weight per area; therefore, it is expected to operate at a higher angle of attack than the aft foil. At a 2.5° angle of attack, the front foil has a coefficient of lift of 0.6 and must have an area of 8,012 mm^2 to support the remaining 30% of the craft.

3.4   Control Surface Design

Several options are available for control surfaces but the desire for scalability motivated the pursuit of a more novel approach towards the control surfaces. The watercraft sits between the typical small-scale remote-control approach of servos with push-pull wires for linkages, and the larger scale hydraulics common to heavy vessels. A more robust but still electric motor-based approach using belts was explored. With electric motors becoming increasing power dense and precise, there is substantial potential for their use in controlling lightweight personal watercraft.
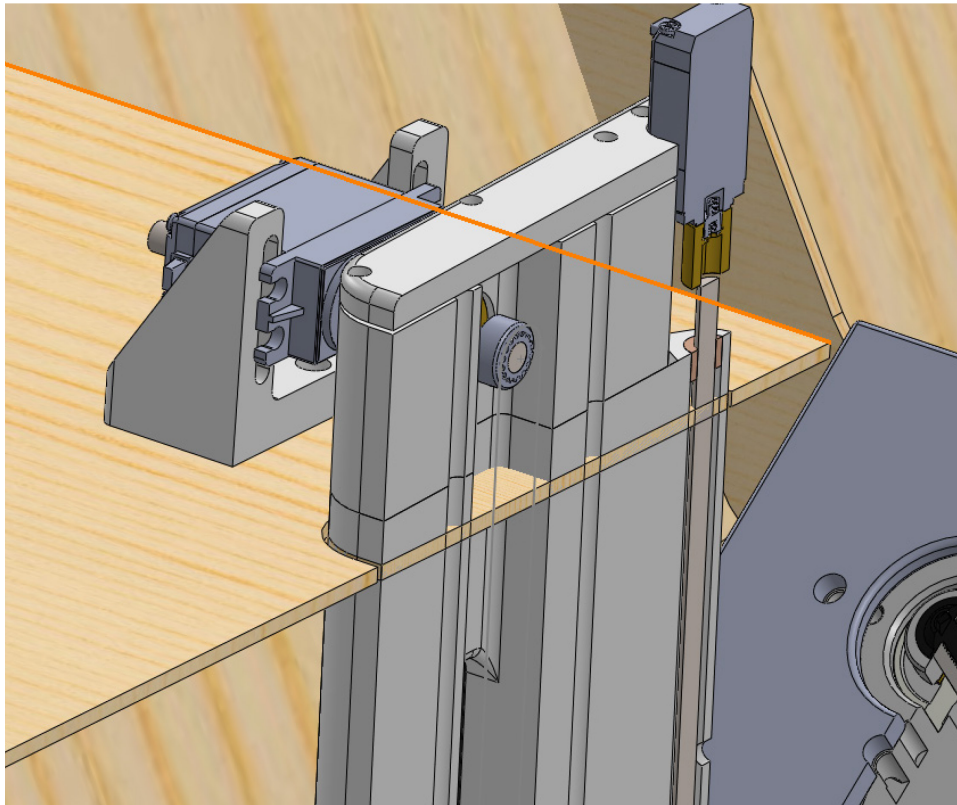

Figure 3.3 The Bilda servo is attached to a shaft to which a pulley is affixed. The belt on this pulley runs through the mast and rotates the control surfaces. Custom tooling was ground by hand to cut internal O-ring seats in the brass bearings that support the pulley shaft. This prevents water from coming up through the mast should the boat ever be flipped.
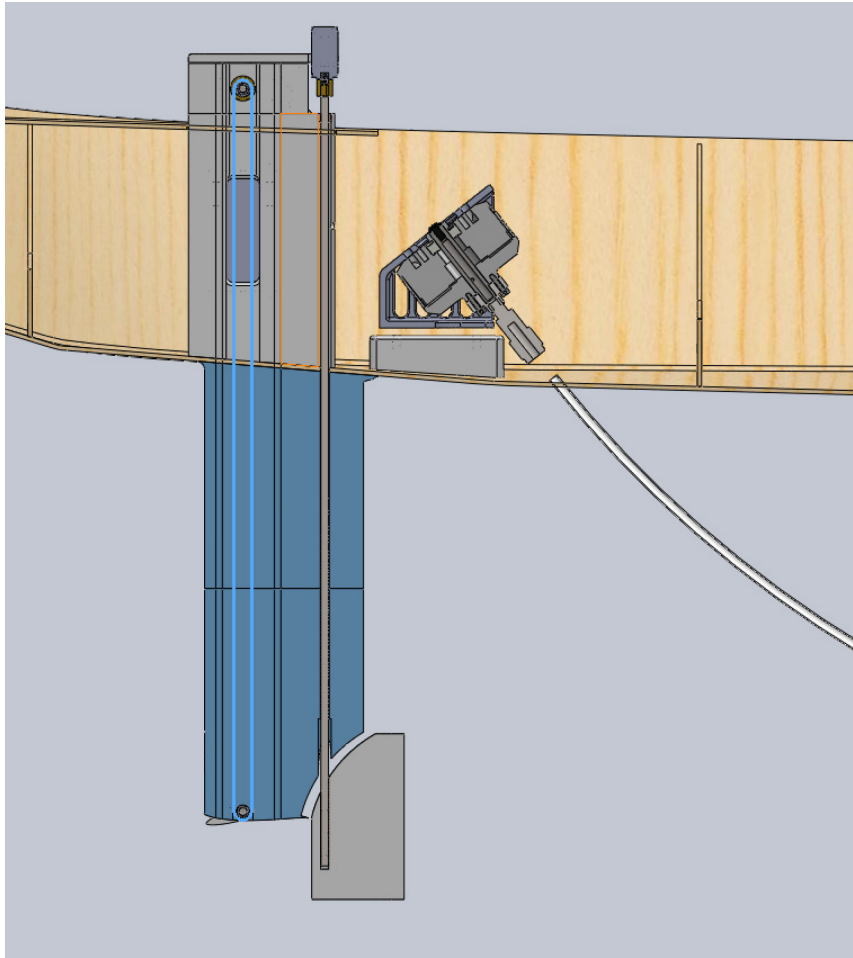
Figure 3.4 Pictured in light blue, the internal belt transmits torque from the servo on the deck to the foil at the bottom of the mast. Also visible is the rudder, which is mounted to the front foil and controlled by another servo on the deck through a stainless-steel rod.

The watercraft is of a size that the hobby servo form factor is still an option for actuating control surfaces. These servos are convenient because they are easily controlled with a pulse width modulation (PWM) signal created by hobby radio transmitters or by microcontrollers. These servos are mounted to the deck to prevent water ingress and connect to the control surfaces through a belt in the mast. Not only does this belt mechanism fit more cleanly into the bottom of the masts, but it has a greater potential for scalability than the hobby control mechanism.

Four control surfaces were created for the watercraft. The rudder is located at the forward mast and is directly rotated by a rod through the mast. The forward foil rotates for pitch control. Either side of the aft foil is equipped with flippers. These have symmetrical foil profiles and can pivot independently to generate lift in the positive or negative direction for roll control. Direct control foils, where the entire foil is rotated, were chosen due to space constraints, ease of construction, and the successful use of these types of foils in naval hydrofoils [3].
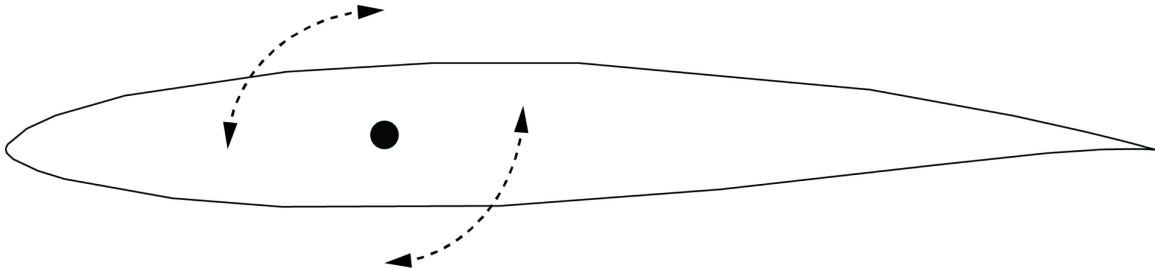
Figure 3.5 The control foils pivot about a shaft mounted through the foil.

The limitations on size due to the confined space was a challenge during the construction and design of the foil control mechanism. The primary issue was belt skipping on the lower pulley. The upper pulleys had more lateral space, allowing for the use of wider, aluminum pulleys. The lower pulleys, however, had to be custom made. The limitation of 3D printing at that scale made for less clearly defined teeth. Both top and bottom pulleys are the same size, so the belt engages with half the teeth at any given time. This is still only an engagement with eight teeth. While the belt itself held up well to the loads on the pulley, it was prone to slipping. Tensioning was achieved in the tight space of the masts by connecting the ends of the belt with a zip tie loop that could then be tightened. Due to the small size of the foils, it was not possible to place the shaft exactly at the center of lift of the control surfaces. As a result, the lift generated by the control foils produced a torque about their rotational axis. Initially, this was not an issue. However, after several rounds of tests the belt on the front foil began to skip teeth. This may have been due to creeping in the belt or zip tie. Future iterations should be tightened, allowed several days to stretch, and then tightened again before the zip tie is clipped and is no longer adjustable. From this experience, the importance of aligning the axis of rotation and the center of buoyancy of flippers was learned. The torque about the shaft from lift was an unexpected danger of using directly controlled foils as control surfaces.

Sufficient command authority over steering was challenging to achieve. Rather than attempting to simulate the complex dynamics of a boat on foil, the rudders were sized experimentally. For simplicity, the rudder is the same foil profile as the mast, extruded and trimmed to fit behind the front foil. The initial rudder provided insufficient steering control. The hull tracks extremely well, maintaining straight line travel is not an issue. Retrieval, however, was complicated by the inability to turn around. A second foil was built, longer and taller than the first. This rudder had some steering ability, though not enough to produce turns of an acceptable radius. Interestingly, it was discovered during testing of the steering that the boat is less stable and more steerable in reverse. Building on the slight success of the second rudder, a third substantially larger rudder was built. This rudder provided adequate steering command but was now so long that the torque on the shaft was able to overcome the connection between the steering shaft and the servo adapter. As a result, the rudder was pushed to a hard stop against the front foil while the watercraft was reversing. In future revision this issue could be resolved by grinding flats on the rudder shaft to better engage with the set screws on the servo adapter.
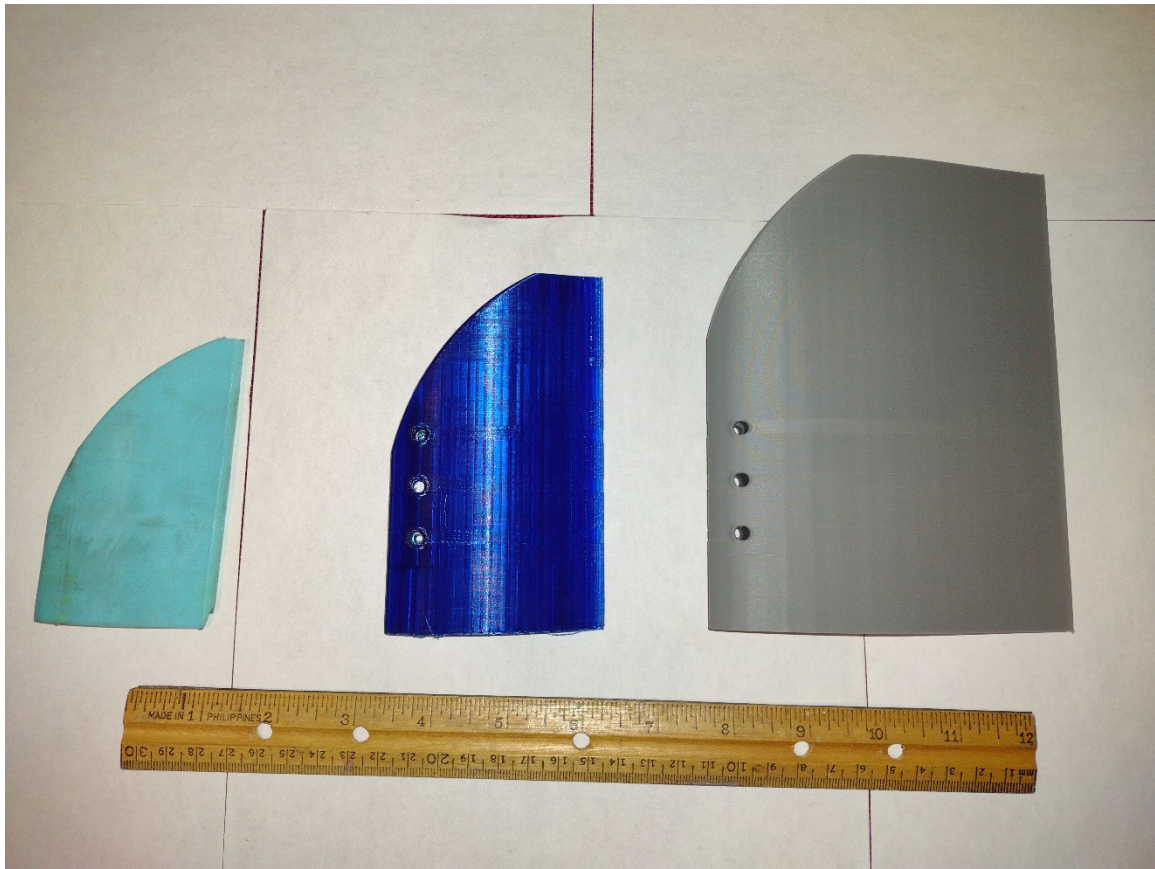
Figure 3.6 Rudders organized left to right chronologically.

Unexpectedly, the largest rudder was able to impart a substantial roll angle on the watercraft. Unlike a traditional watercraft, the rudder must maintain immersion during foiling and is therefore mounted below the foil height. The result is significantly more torque in the roll axis than the rudder on a conventional watercraft. This result, while unexpected, reveals the importance of the rudder, in conjunction with the aft flippers, in controlling roll.

4 Construction
4.1   Hull Construction
The hull of the craft is based on a utility garvey designed by Weston Farmer called the Wanigan [12]. This is a fifteen-foot work boat as originally designed, but it was rescaled to only five feet. Linearly scaling boat plans is not a hydrodynamically sound technique as the hydraulic forces are nonlinear. Nevertheless, the wide and stable but relatively deep V-hull performed adequately when rescaled.

The stitch and glue technique is a method of wooden boat construction that involves "stitching" together 2D plywood panels into a 3D shape and gluing the seams with thickened epoxy reinforced with fiberglass tape. This method was selected as appropriate for the construction of the hull for several reasons, most importantly the lack of need for a mold and the compatibility with the foil construction methods. The hull was designed in the Solidworks CAD software and 2D sections of the hull were unwrapped

from the 3D hull model. These sections were then exported to the HSMWorks CAM tool and cut on a large form-factor CNC router. 1/8in cabinet grade plywood was used for its high strength to weight ratio, low cost, and allowable bend radius before cracking.

Figure 4.1 The 1/8in plywood is fixtured to spoilboard with small screws and cut with a ShopSabre CNC router.

Holes were then manually drilled along the mating edges at approximately 1in spacing, with tighter spacing at smaller bend radii. Short lengths of copper wire were looped through these holes, lacing the panels, and establishing the shape of the hull. The shape of the hull was further refined by gluing in bulkhead pieces with cyanoacrylate glue.
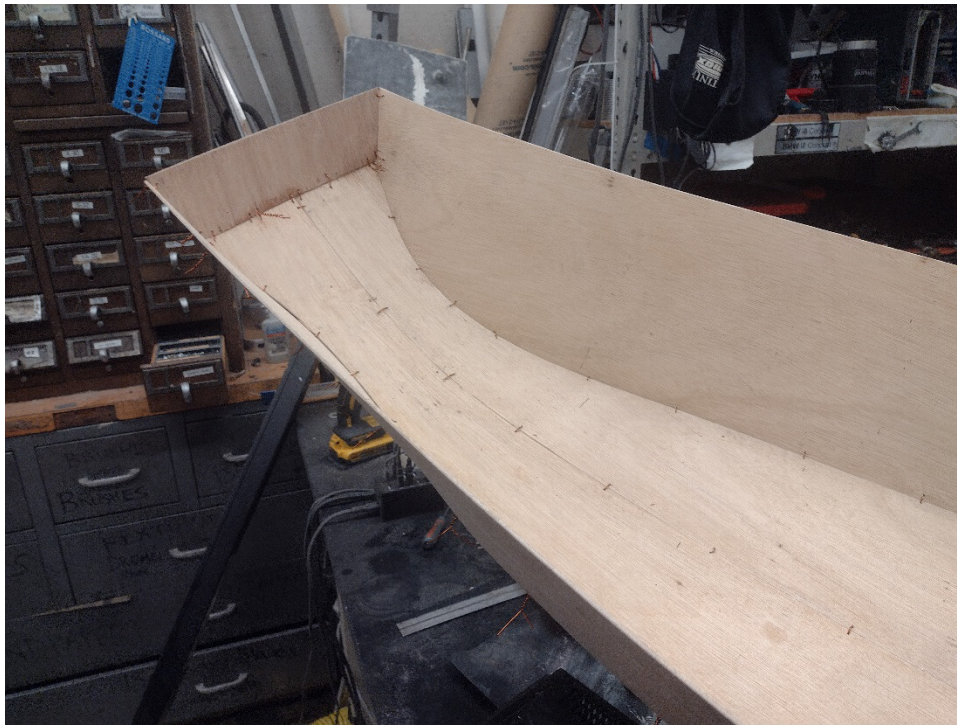
Figure 4.2 Thin copper wire holds the panels together.
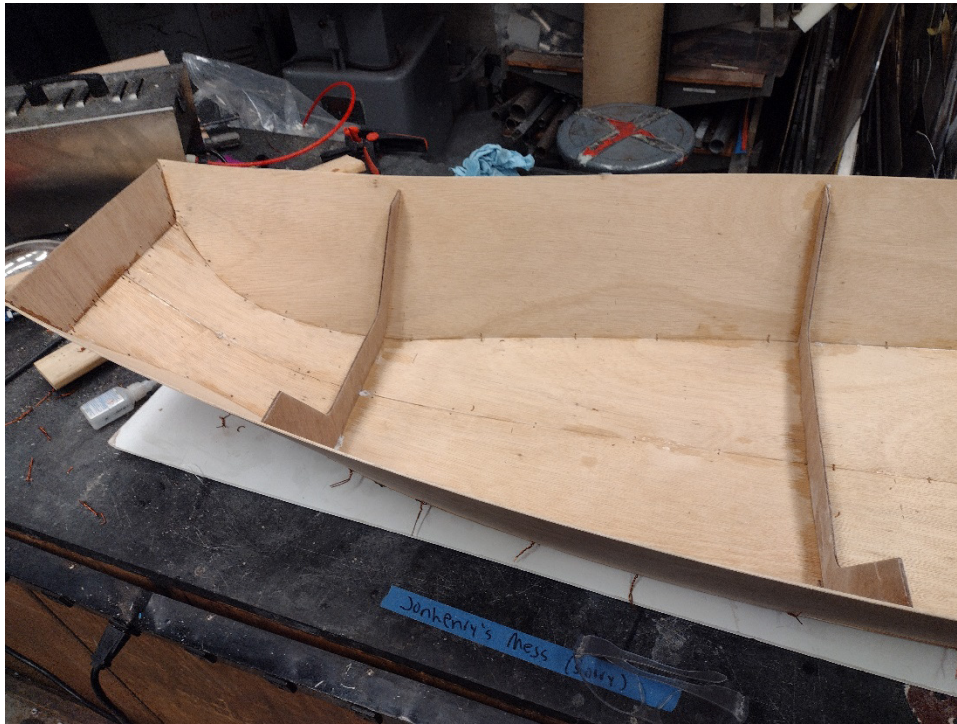
Figure 4.3 Cyanoacrylate glue is visible at the joints Bulkheads help form the 3D hull shape.

The seams in the hull were temporarily fixed with cyanoacrylate glue and the copper wire was removed.

Figure 4.4 Fiberglass tape, visible in white, before being wetted out with epoxy. This tape will strengthen the joints.

A fillet of two-part epoxy resin thickened with micro balloons and fumed silica was applied to each seam. 1.5in fiberglass tape was cut to length, wetted out with epoxy, and applied over the uncured epoxy seams. It was learned that wetting out the fiberglass tape prior to applying it to the seams was prone to trapping bubbles. The uncured fillet provided a poor backing when attempting to push out bubbles, and efforts to mechanically squeegee the air out of the tape tended to simply push the fillet away instead. To avoid air bubbles, either epoxy must be applied over dry tape, or wetted out tape must be applied over cured epoxy. Regardless, this defect appears to be mostly cosmetic, though it will have to be monitored for failure over time.

The result is a highly durable, lightweight hull. However, it is not waterproof. The plywood adhesive is not rated for exposure to water, which can lead to delamination if measures are not taken to seal the hull. For waterproofing, abrasion resistance, and stiffness, a layer of fiberglass is applied to the underside of the hull with an epoxy surfboard resin.

Figure 4.5 Where wetted out with epoxy, the fiberglass is clear.

4.2   Hydrofoil Construction

3D printed masts and hydrofoils with fiberglass skin were built to experimentally explore their feasibility in this type of watercraft. Modeling these types of structures is difficult with traditional FEA techniques due to the high anisotropy of the composite structure and the 3D printed plastic itself, combined with the complex fluid dynamic forces to which the masts may be subjected. FDM printing is well suited to producing complex, smooth geometries of hydrodynamic surfaces. However, FDM 3D prints are highly permeable and would become waterlogged if used alone. Instead, the 3D printed plastic was covered with an epoxy fiberglass composite skin. This skin also adds substantial strength to the otherwise overly brittle and flexible PLA plastic.

The 3D printed foils were prepared for fiberglassing with heavy sanding and filleting to remove sharp transitions. The foils were assembled from multiple pieces due to the size limitations of the 3D printer and glued together with epoxy adhesive at simple butt joints.
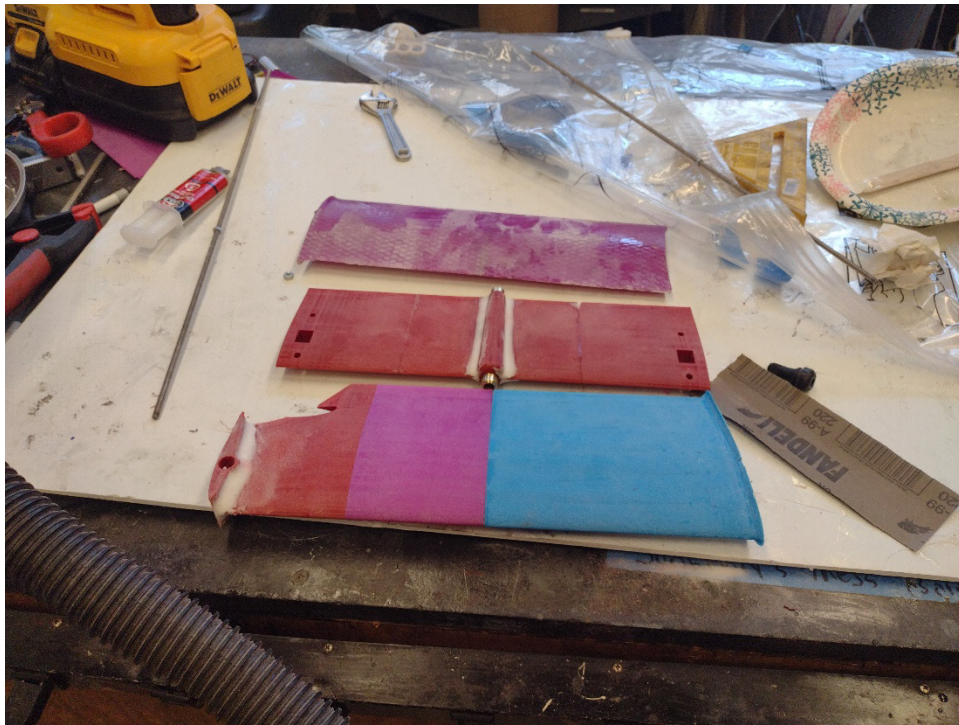
Figure 4.6 From top to bottom: finished aft mast, glued and faired aft foil, glued and faired forward mast. Notice the brass tube in the rear foil. This is a simple bearing that will support the drive shaft.

Once prepared, two layers of fiberglass-epoxy composite were applied to both sides of the foils and masts. This process was done using the vacuum bagging technique, which involves layering a release layer and a permeable, breather layer on top of the fiberglass. This preparation is placed into a bag and a vacuum pulled, applying even clamping across the fiberglass with atmospheric pressure. Space saving compression bags were used for this purpose.
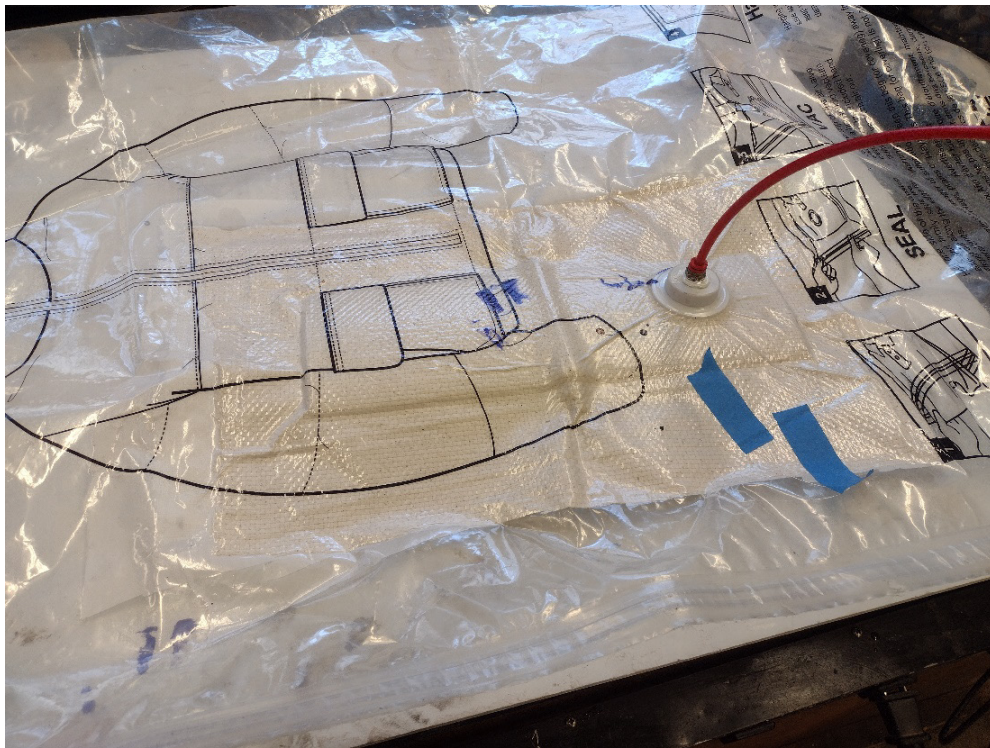
Figure 4.7 The top breather layer is visible through the vacuum bag. This layer allows air to escape around the foil during vacuuming.
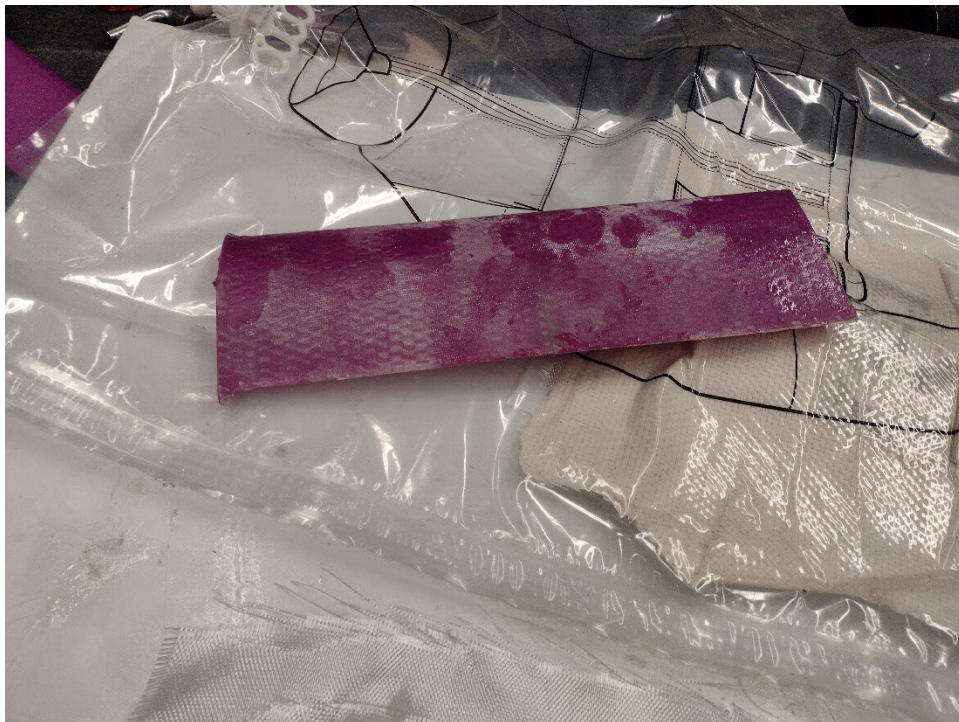
Figure 4.8 A cured fiberglass aft mast. Some texture is left from the breather layer that will later be removed by hand with a palm sander.

Finally, the foils were glued to the hull with epoxy adhesive. To reinforce the joint, a fillet of epoxy and chopped fiberglass was applied at the seams. This formed an unexpectedly strong bond to the boat hull. This is likely due to the compatibility of epoxy with itself, and the weave of the fiberglass providing a keyed surface to which the epoxy mechanically connected.

Figure 4.9 Note the PTFE tube attached to the rear foil. This will later penetrate the hull and forms a smooth, low friction liner in which the flex shaft will run.

Finally, the hull was painted with Rust-Oleum Marine Topside paint to smooth the surface and improve waterproofing.
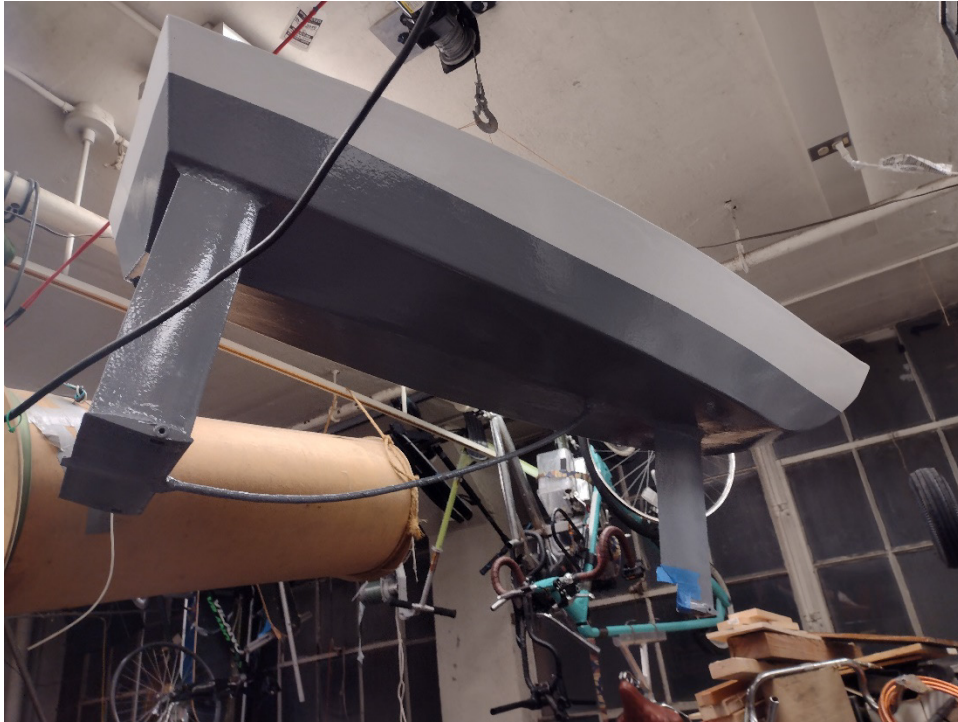
Figure 4.10 Here the PTFE liner has been reinforced with fiberglass and affixed where it penetrates the hull.

Some challenges were encountered in fiberglassing the 3D printed structures. Adhesion was surprisingly poor between the PLA structures and the fiberglass sheath, particularly at the tight radius at the leading and lagging edges of the foil profiles. This was resolved to some extent by filling with epoxy and sanding down to shape, but the imperfect foils likely affect the generated lift and drag. This may be a useful finding when selecting 3D printing plastic materials for epoxy compatibility. Even with this issue, the masts and hydrofoils are exceptionally robust. The foils and masts have held up to repeated impacts with underwater structures, and to rough handling out of the water. No water ingress was detectable after multiple hours in the water.

4.3   Flex Drive

This project explores the use of a flexible drive shaft for propulsion. This drive system was chosen because it allows the motor to be placed in the watertight hull without the use of complex gears typically used on hydrofoils to redirect the shaft. A more conventional rigid shaft at an angle is also not possible, because the vertical distance between the prop and the motor would put too extreme of an angle on the shaft. While flex shafts are used extensively on hobby sized watercraft, they are less explored on vehicles as sizeable as the watercraft described in this work.
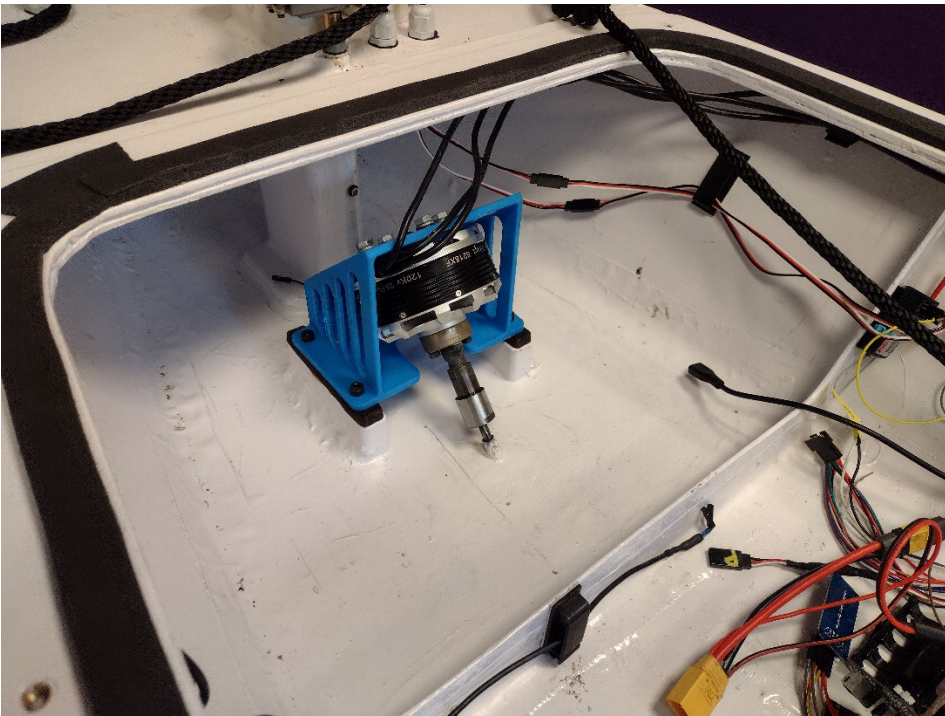
Figure 4.11 The flex shaft is driven by a brushless outrunner motor intended for heavy lift drones. This is a sensorless motor, which works well in propellor driven vehicles because startup torque is low.

The flex shaft cuts down significantly on complexity by simply threading through a PTFE tube. Some concerns were had with heat dissipation from friction inside of the tube, as the polymer can soften and bind when hot. However, field testing has not resulted in noticeable temperature differences and there is no visual degradation of the tube.

Figure 4.12 The end of the drive shaft is a stack of a locknut, prop, coupler, thrust washer, thrust bearing, thrust washer, and O-ring. Marine grease lubricates the shaft and O-ring and prevents the ingress of water.

The drive shaft was modified from a power tool flex shaft. The motor end of the shaft was brazed closed to prevent fraying. A rigid section was welded to the propellor side of the shaft, to be supported by the brass bushing in the aft foil, and a coupler was brazed on. This coupler mechanically transmits torque to the prop. The prop is retained by a locknut that threads onto the rigid section of the shaft. This represents an improvement over the original version, which used setscrews and slipped laterally down the shaft while the propellor was running in reverse.

4.4   Waterproofing

Waterproofing was completed mostly through the liberal application of grease and sensible placement of the non-waterproof components. When possible, components were mounted above the hull to prevent leaking onto the electrical components. Placing the motor in the hull was unavoidable both for structural integrity and to keep the radius of the flex shaft large to cut down on friction. Where shafts were run through significant lengths, the tubes were simply filled with waterproof marine grease to serve as simple stuffing boxes. Experimentally, water was able to work itself up the flex shaft tube by

approximately 10 cm, but not in significant quantities and no leaking was ever found into the hull.

The feasibility of waterproofing the mast and belt mechanism was explored. Since the servos are not waterproof, measures were taken to keep them out of the water. The servos are mounted above the deck, keeping them out of water. The servos were originally planned to be fully enclosed because overturning was a major concern early in the project. As it turns out, the hull is extremely stable and at no point during testing did the watercraft approach flipping. Before the stability was apparent, dynamic seals were designed to keep water from leaking into the servo enclosures. Originally, these seals were intended to be mounted to the bottom of the masts. However, tight constraints on space and the need to access the pulleys necessitated their installation at the servo shaft instead.

Creating O-ring seals was unexpectedly challenging. The O-rings must be sized appropriately for the servo rod, and the groove must be appropriately sized for minimum compression of the O-ring. The Parker Oring eHandbook was consulted for this sizing [13]. A custom tool was carved freehand with a rotary grinding tool from a HSS blank. This was then used as a form tool in a lathe to cut the O-ring groove. The groove was cut into a brass cylinder that was reamed to tightly fit the servo shaft and act as a simple bearing. It was then glued into the upper mast.

Figure 4.13 The 6mm stainless steel shaft rotates with little resistance in the brass cable gland. The brass is chosen for its low friction properties as a plain bearing, and for its resistance to corrosion in the presence of water.

Surprising, the proper fit between shaft, O-ring, and O-ring gland specifies only a few percentages of squish to form a good seal. This means that very little friction is added to the system through the inclusion of the O-ring. Producing watertight dynamic seals appears to be reasonable in a home shop with no specialized equipment, even with hand-carved tooling.
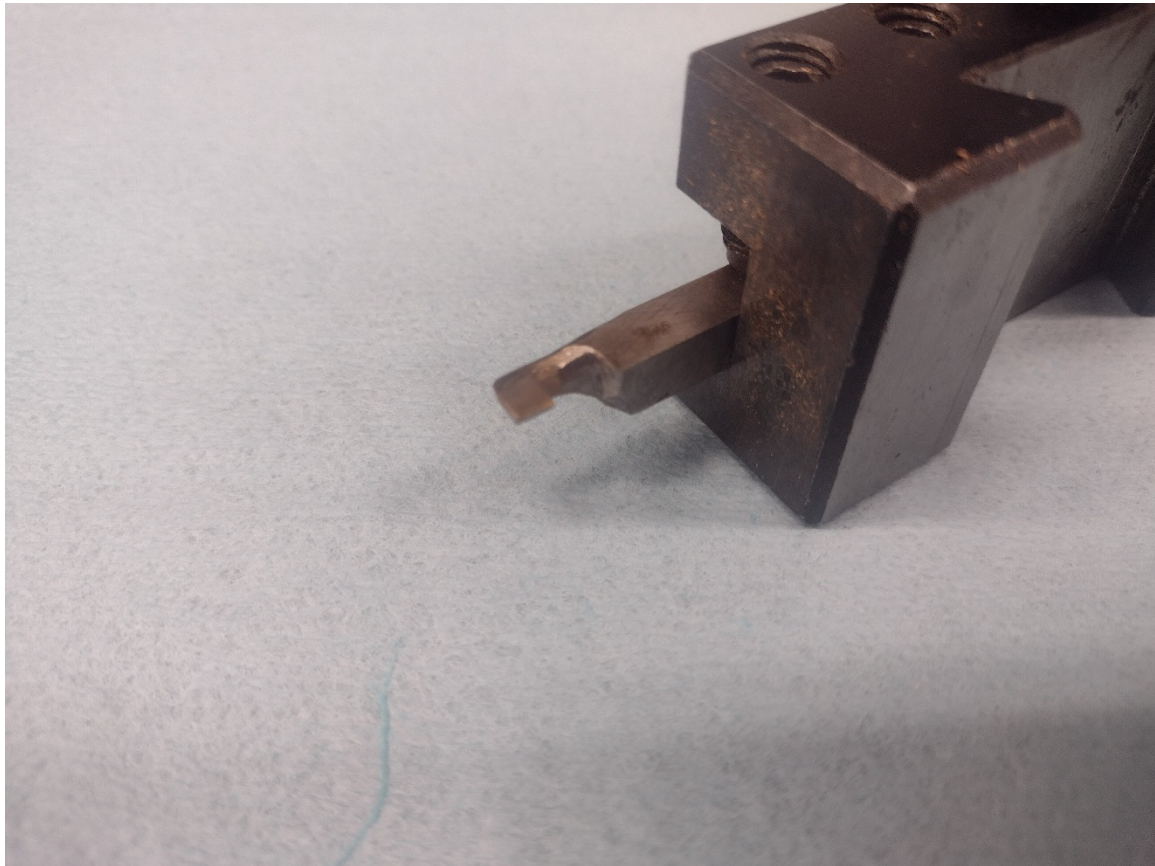
Figure 4.14 Pictured is the high speed steel tool clamped in a lathe toolpost. The cutting edge is relieved, and a substantial throat was cut behind the tool to allow the tool to reach into the bore of the O-ring gland.

4.5 Electronics

An Adafruit Feather ESP32-S3 was chosen for use due to its availability, ease of use, and powerful feature set. One goal of the overall project was to build familiarity with the ESP32 in a C++ environment. Providing all four servos with the correct PWM control signal directly from the ESP32 proved difficult. Instead, a PCA9685 16 channel servo driver controlled over IIC was used to interface with the servos. The primary microcontroller also communicates with a BNO055 IMU for angle and angle rate data. Height data are provided by a pair of JSN-SR04T ultrasonic sensors. It was discovered that these sensors miss an unacceptable percentage of pings when used more often than every 0.01 seconds. While attempting to increase the ping rate of the sensors, a method of averaging sensor data was devised, and missed pings were reassigned to an average of the last viable values. This was more reasonable, but it is likely that multiple sensors will need to be used to increase speed and reliability. Power is provided to the servos by a

step-down converter from the 48v nominal battery system to 12v. This is then further adjusted to the 5v necessary for the servos and the HiLetgo micro-SD card adapter with a buck converter.

A hobby 6 channel transmitter and a receiver are used to communicate with the microcontroller and control the steering and throttle on the watercraft. A level shifter resolves the communication voltage mismatch between the 5v receiver and 3v ESP32. The motor is driven by a Flipsky 75100 motor controller.

5 Experimental Design

5.1 Frequency Sweep

A frequency sweep was performed to characterize the roll response of the watercraft in response to the pitch angles of the aft flippers. A large amplitude pitch in the flippers of 15 degrees was chosen to ensure that the frequency response was distinguishable from the noise caused by testing in an uncontrollable body of water. The Bilda 2000 series speed servos are used for control of the roll flippers move at 90 rpm under no load [14]. This limits the maximum testable frequency to 113 rad/s before the servos can no longer keep up with the commanded position. The lower testable frequency is determined by the range of the transmitter. The watercraft must not move so far away from the transmitter that it loses connection. A reasonable starting point of 1 rad/s was chosen.

The microcontroller running the boat is single threaded, it is unable to run multiple operations simultaneously. The entire loop must run sufficiently fast to adequately control the servos while still saving data about the commanded position and response of the roll control. Multiple configurations of the code were explored to produce more efficient software including the use of non-blocking code and buffering techniques in data taking. The first set of code continuously saved roll angle, frequency, time, and commanded flipper angle. This was fine for low frequencies, but at more than about 6 radians per second the sinusoidal angle commanded to the flippers began to look less sinusoidal.

Some investigation of the code revealed that the code was hanging when saving to the SD card. A buffer was needed to reduce the frequency of saving to the SD card. The ESP32-S3 microcontroller used in the boat has more than enough storage space to hang onto the entire set of data corresponding to each frequency. However, the string storing the data in the ESP32 had to be concatenated with each new set of data. The first attempt at saving to the SD card only when changing testing frequency lagged worse than when saving continuously to the SD card. The fix for this turned out to be simple. The format "string = string + newstring" runs substantially slower than "string += newstring". This single line change was sufficient to completely solve the lagging issues. The resulting control effort follows smooth curves with jumps only when saving to the SD card.
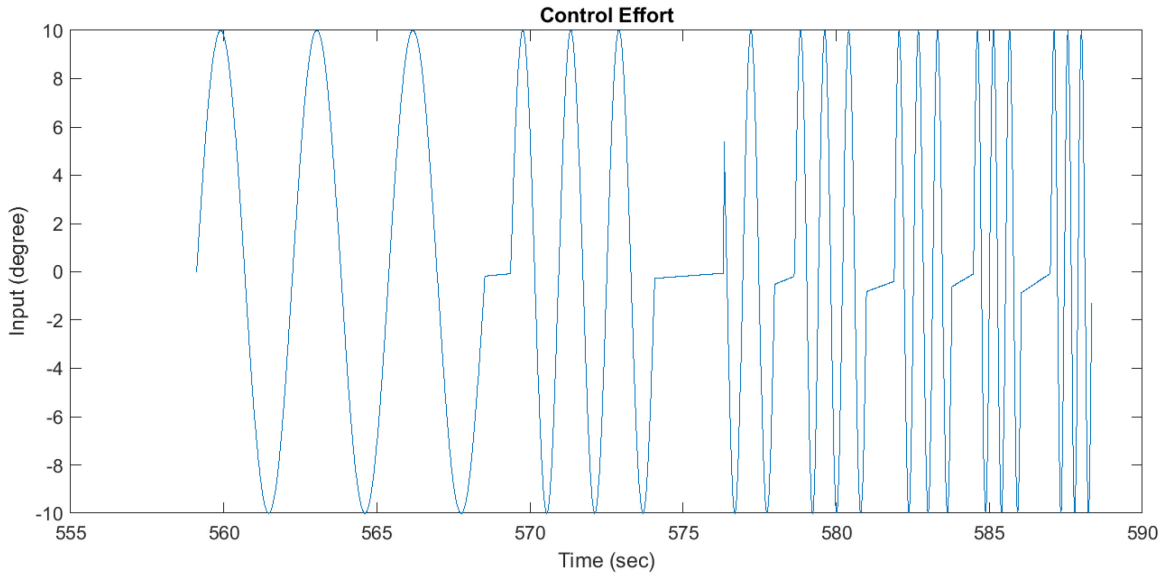
Figure 5.1 Note the horizontal or near horizontal sections between the sinusoidal waves. These represent the delay due to the time needed to save to the SD card.

6 Conclusions and Future Work

6.1 Characterization and Controls

Ultimately, the characterization of the watercraft was not completed. The limited range of the transmitter limited data acquisition to a short time frame. One solution might be to individually test the response, manually stepping through frequencies and visually determining the phase and magnitude at each frequency. It would also be important to step through the magnitude of the commanded roll angle. For linear control theory to be applicable, a regime must be found where increasing the magnitude of the input changes the frequency response linearly. Most likely, this would lie at some small input angle.

After acquiring a frequency response, control theory could be applied. The results of Talha Ulusoy suggest a proportional derivative (PD) controller could be effective in reducing roll [4].

6.2 Power and Drag

Rather than attempt to model the drag of the complex semi-supported planing hull, the watercraft was built with a ten-kilowatt motor with the assumption that this would be more than adequate to achieve foiling speed. The drive train proved to be inadequate in propelling the watercraft to foiling speeds. It is possible that the motor controller is limiting current to the motor unexpectedly. It is also possible that the propellor is too inefficient to adequately propel the craft. Some experimentation was done to adjust the pitch and diameter of the propeller with minor gains in speed, but more work could be done in designing an efficient propellor. Future testing would benefit from data logging from the motor controller to determine the bottleneck in power delivery.

There is also room for characterizing the drag of the watercraft. Most simply, this could be done by dragging the watercraft behind a motorboat on a tow cable equipped with a force sensor. This tension would be equivalent to the drag produced by the boat at

speed. With a known drag, it would be possible to determine the correct drivetrain to lift the boat onto foil.

6.3   Conclusion

While the watercraft has not yet foiled, theory suggests that the correct powertrain and controls would allow for a cruising speed on foil at only 4 m/s. The structure of the hydrofoil held up well with no leaking, damage, or significant deflection during testing. More work is needed on the power train and steering system, and there remain some unresolved issues with the tensioning in the belt-controlled control surfaces. The novel mast integrated control surfaces are promising but would benefit from more robust pulleys to increase the tolerable torques on the controllable foiling surfaces. The waterproofing of the control surfaces with O-ring glands has been successful even with home-shop quality machining and equipment. Minor changes to the hardware would go a long way towards improving performance. For example, upgrading to a more watercraft specific transmitter would increase the time during which tests can be run without needing to retrieve the craft. Major improvements were made to the vehicles software through the course of testing, resulting in smoother servo control and substantially improved response times. However, more testing is needed to characterize the response of the craft, and experimental tuning will be needed to develop the control system.

Figure 6.1 The completed vessel.

7 References

[1]   Acosta, A. J., 1973, "Hydrofoils and Hydrofoil Craft," Annu. Rev. Fluid Mech., **5**(1), pp. 161–184.

[2]   Liu, S., Xu, C., and Zhang, L., 2017, "Hierarchical Robust Path Following Control of Fully Submerged Hydrofoil Vessels," IEEE Access, **5**, pp. 21472–21487.

[3]   O'Neill, W. C. and R.J Johnston, 1974, "The Development of Automatic Control Systems for Hydrofoil Craft," Hydrofoil Dev. P- Gram Off. Nav. Ship Res. Dev. Cent.

[4]   Ulusoy, T., 2004, "Roll Stabilization for Fast Monohulls by Using Passive and Active Lifting Appendages," Thesis, Massachusetts Institute of Technology.

[5]   Mahmud, Md. S., 2015, "The Applicability of Hydrofoils as a Ship Control Device," J. Mar. Sci. Appl., **14**(3), pp. 244–249.

[6]   Hoerner, S. F., and Borst, H. V., 1975, "Fluid-Dynamic Lift: Practical Information on Aerodynamic and Hydrodynamic Lift," NASA STIRecon Tech. Rep. A, **76**, p. 32167.

[7]   Faltinsen, O. M., 2005, *Hydrodynamics of High-Speed Marine Vehicles*, Cambridge University Press.

[8]   Mircea, L., Cristian-George, C., and Gheorghe, R., 2018, "The Absolute Stabilization and Optimal Control of Hydrofoil Watercrafts," INCAS Bull., **10**(4), pp. 85–96.

[9]   Hoerner, S. F., 1965, "Fluid Dynamic Drag, Published by the Author," Midl. Park NJ, pp. 16–35.

[10]   "EPPLER E838 HYDROFOIL AIRFOIL (E838-Il)" [Online]. Available: http://airfoiltools.com/airfoil/details?airfoil=e838-il. [Accessed: 02-Jan-2023].

[11]   "H105H" [Online]. Available: http://www.tspeer.com/Hydrofoils/h105/h105.htm. [Accessed: 29-Apr-2023].

[12]   "Wanigan (Free Plans)," Duckworks Boat Build. Supply [Online]. Available: https://duckworks.com/wanigan-free-plans/. [Accessed: 08-May-2023].

[13]   "Rotary O-Ring Seal Gland Design," Park. Hannifin Corp. [Online]. Available: https://promo.parker.com/portal/site/PROMOSITE/menuitem.0a9e0999bb064e495e2f3ef 7427ad1ca/?vgnextoid=8bf375fb40d1f410VgnVCM100000200c1dacRCRD&vgnextcha nnel=ad625af3ccedd410VgnVCM100000200c1dacRCRD&vgnextfmt=EN. [Accessed: 10-May-2023].

[14]   "2000 Series Dual Mode Servo (25-3, Speed)," goBILDA [Online]. Available: https://www.gobilda.com/2000-series-dual-mode-servo-25-3-speed/. [Accessed: 01-May-2023].